A first-principles study of the lattice distortion around a solute atom in BCC lithium

1995 J. Phys.: Condens. Matter 7 2461

(http://iopscience.iop.org/0953-8984/7/12/010)

J. Phys.: Condens. Matter 7 (1995) 2461–2471. Printed in the UK

A first-principles study of the lattice distortion around a solute atom in BCC lithium

P T Salo, K Kokko, R Laihia and K Mansikka
Department of Physics, University of Turku, FIN-20500 Turku, Finland

Received 5 December 1994, in final form 7 February 1995

Abstract. In this paper, we study the effect that the lattice distortion around a solute atom (Na, Mg, Al) has on the electronic and mechanical properties of BCC Li using the first-principles structural optimization method. In the present calculations, a 54-site supercell is used to get a better insight into the long-range behaviour of the lattice distortion around a solute atom. The results show that the behaviour of the first-nearest-neighbouring Li shell around a solute atom in all cases investigated is similar to that obtained in the corresponding 16-site supercell calculations. The distortion has, for instance, an effect on the average atomic volume, bulk modulus and heat of formation of Li alloys. From the present calculations, together with our previous studies, we deduce also the concentration dependence of these quantities. For example, the calculated average atomic volume and bulk modulus of dilute Li–Mg alloys, as a function of Mg concentration, agree qualitatively very well with experimental results. Furthermore, the pressure dependence of the lattice distortion is found to be rather important. Our results also predict that the solubility of Na in BCC Li under pressure above 50 kbar is possible.

1. Introduction

In recent years, a number of investigations have been performed on Li metal and Li-based alloys. Also alloys and compounds that contain Li have been studied lately: for instance, Al–Li systems have been investigated both theoretically and experimentally because of their technological potential for aerospace materials. The theoretical studies of Li-based materials are of great value since experimental investigations are quite difficult to perform due to the high chemical activity of Li. Summarizing from the above, we mention some of the latest theoretical investigations on Li and Li alloys [1–9].

In this work, we study the effects that the lattice distortion around a solute atom (Na, Mg, Al) has on the electronic and mechanical properties of BCC Li using the first-principles molecular dynamics method [10]. This method enables us to optimize the crystal structure which in turn makes it possible to investigate how lattice distortion around a solute atom affects the physical properties of an alloy. Solids that contain impurities can be considered as dilute alloys, although in our case we limit considerations to ordered structures. We study these Li systems since the solute atoms in question differ from each other in many respects and the alloys formed are quite different in nature, thus giving a good general idea of the properties of Li alloys. The solid solubility of Mg in BCC Li is high, whereas Na has only very little terminal solid solubility in Li with no known intermediate phases. In the Li–Al system two intermediate phases exist. Although the Li–Na alloys exist only in a homogeneous liquid region [11] or perhaps at high pressure, we may consider a Na solute atom as a substitutional impurity and, thereby, get some systematic knowledge of the effects of various properties of solute atoms, such as valence, atomic size, electronegativity etc.

0953-8984/95/122461+11$19.50

In our previous investigations [12, 13], we discussed the effect of lattice distortion around a solute atom on, e.g. bulk modulus and band structure in Li alloys using a 16-site supercell. With this supercell, however, the long-range behaviour of the lattice distortion and the effect of isolated impurities cannot be studied properly. In the present work the structural and cohesive properties of Li–X (X = Na, Mg, Al) systems are studied using a 54-site supercell (containing 27 conventional BCC cells). From the present study, together with our previous studies, we also obtain more detailed knowledge of the effect of a lattice distortion on different quantities as a function of solute atom concentration. Furthermore, the influence of pressure on lattice distortion, bulk modulus and heat of formation is presented. The obtained results are compared to those of other theoretical investigations and experimental data when available.

2. Calculational procedure

The electronic structure calculation is based on the density functional theory including the local density approximation [14, 15] with the Wigner interpolation formula [16] for the exchange and correlation. The wave functions of the valence electrons are expanded using the plane-wave basis and the effects of ionic cores are introduced using pseudopotentials. Norm-conserving pseudopotentials are obtained by following the prescription of Bachelet *et al* [17], except for the pseudopotentials corresponding to the unoccupied states of the neutral atoms, which are obtained by Hamann's scheme [18]. The d part is treated as a local potential and the pseudopotentials are transformed into a separable form as suggested by Kleinman and Bylander [19]. The partial core correction [20] is included in the pseudopotentials of Li, Na and Mg [21].

The optimization of the electronic and ionic degrees of freedom is performed by using the first-principles molecular dynamics [10], where the modified steepest-descent (MSD) type of algorithm [22] is used to optimize the electronic part. The $Li_{53}X$ alloys used here are fully ordered systems, implying that it is justified to assume that the MSD method works well in our case (see [23]). In the vacancy calculation of the 54-site Li supercell, Benedek *et al* [3] stated that the calculations with the MSD method take about 150 iterations to reach satisfactory convergence, a finding which is also confirmed in our electronic structure calculations for fixed BCC positions. The ionic motion is calculated using ordinary molecular dynamics with the Hellmann–Feynman forces [24]. The method is described in greater detail in [25, 26].

We have made test calculations to check the effects of various computational parameters for the cut-off energy (E_{cut}), number of k-points (N_k), Gaussian broadening near the Fermi level and the number of orbitals needed. The convergences of energy and forces have been tested with different combinations of parameters to optimize the calculational procedure. The Schrödinger equation is solved self-consistently within a plane-wave basis. This basis includes all plane waves with an energy less than a certain cut-off energy. In order to determine a proper value for this, the total energy and forces acting on the atoms, fixed at their ideal BCC positions, have been calculated for $Li_{53}Al$ as a function of E_{cut}. The cut-off energy of the plane-wave basis 10.0 Ryd is used since this value gives good enough convergence for total energy and forces. The same kind of procedure has also been followed for the total number of k-points. The energy summation has been tested with both the ordinary and special k-point [27] sampling using a Gaussian-type broadening scheme [28] near the Fermi level with different widths. Elsässer *et al* [29] have shown that the Gaussian broadening is variational with respect to fractional occupation numbers. In metallic systems

the width must be large enough to avoid the possible abrupt interchanges between the occupied and unoccupied states that reduce the convergence of the calculations. Special k-points have been found to be superior to ordinary k-points, and the tests show that it is enough to use four special k-points in the irreducible wedge of the simple cubic Brillouin zone (SC IBZ). With this k-mesh the best choice for the width used in the $Li_{53}X$ calculations is about 2 mRyd in which case 32 orbitals are needed. More details of these test calculations are available in [30].

In the structural optimization procedure, 150 iterations of electronic structure calculation with fixed atomic positions are performed before the atoms are allowed to move according to the forces. The optimized structure could then be reached by following the forces during the relaxation process. Since there are six relaxing shells of Li atoms neighbouring a solute atom, the calculations would be very time consuming, unless we made them less so by modifying the input data of atomic positions 'by hand' as suggested by the forces in the ideal BCC structure. After that the structure of Li alloys is optimized by allowing the atoms to move according to the forces in the molecular dynamics calculation.

In our previous studies the convergence criterion for forces acting on atoms was 1.0 mRyd/a_0 (a_0 is the Bohr radius). That is quite a satisfactory limit for calculations in the 16-site supercell where there is only one degree of freedom, i.e. there is only one atomic shell that can freely relax. But in the 54-site supercell, where there are six degrees of freedom and where the displacements of atoms may also influence one another, the above criterion would not be satisfactory to get a reliable conception of the lattice distortion around an impurity. Thus, the convergence criterion for forces has been tightened and 0.2 mRyd/a_0 has been found to be sufficient for $Li_{53}X$ systems with the above-mentioned choice of computational parameters. However, the effect of different convergence criteria for forces is not significant when calculating the values of total energy, equilibrium lattice parameter and bulk modulus.

3. Results and discussion

The substitution of a host atom by an impurity atom produces a local strain in the crystal lattice. The lattice distortion in BCC Li induced by a substitutional solute atom (Na, Mg, Al) has been studied earlier using a 16-site supercell [12, 13]. With this supercell, the lowest possible solute atom concentration which can be used in calculations is about 6%. In order to investigate the dependence of this distortion on the solute atom concentration, the unit cell has been increased in the present calculations to contain 54 atoms. Using this larger unit cell it is possible to simulate solutions of less than 2% solute atom concentration. By considering the results for 6% and 2% solutions correspondingly it is also possible to obtain some predictions for the effects of isolated impurities.

In the present study, the total energies of Li_{54} and $Li_{53}X$ have been calculated with four different lattice parameters for ideal BCC and optimized structures in the neighbourhood of the total energy minimum. After having done the fit presented by Banerjea and Smith [31] we have calculated the equilibrium lattice constant and bulk modulus from the obtained total energy curve. The effects of pressure on lattice distortion, bulk modulus and formation energy can also be determined from that curve.

3.1. Lattice distortion due to a solute atom

The displacements of Li atoms in the first six neighbouring atomic shells that surround a solute atom in $Li_{53}X$ (X = Na, Mg, Al) systems are presented in figures 1, 2 and

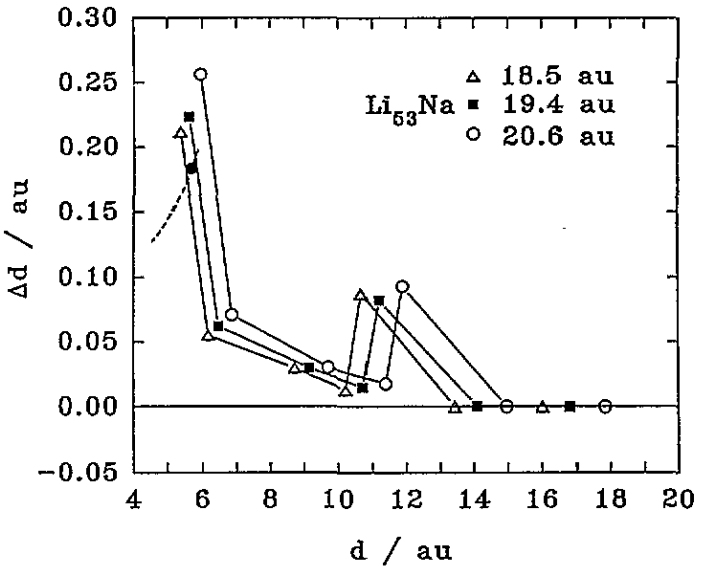

Figure 1. The calculated displacements of neighbouring Li shells surrounding a Na solute atom in the $Li_{53}Na$ supercell. The displacements (Δd) versus the distance (d) from a Na solute atom are presented with three different lattice parameters (black squares represent the equilibrium structure). For the sake of comparison, we also include the guideline from the results of $Li_{15}Na$ (dashed curve, black circle indicating the zero-pressure value). The distance d refers to the ideal *BCC position of the corresponding neighbour atom.*

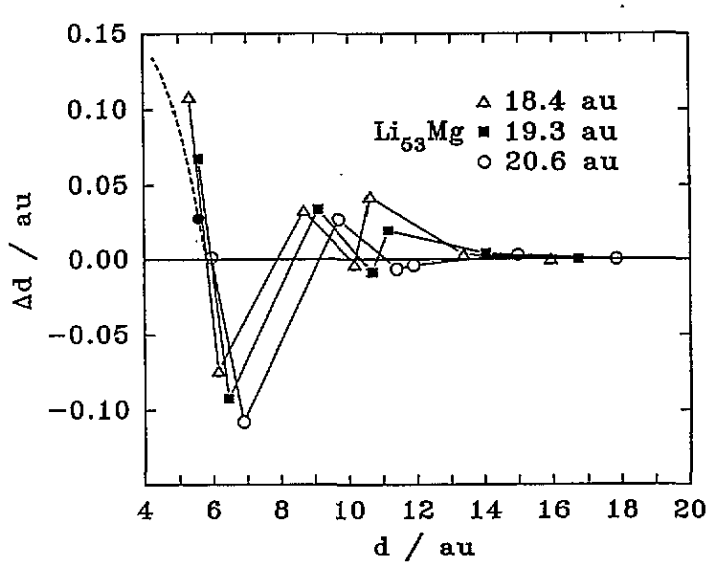

Figure 2. The corresponding data for $Li_{53}Mg$ as explained in the caption of figure 1.

3, respectively. In spite of the fact that the degrees of freedom of the relaxation have increased from one to six compared to the 16-atom unit cell, the relaxation in the first-

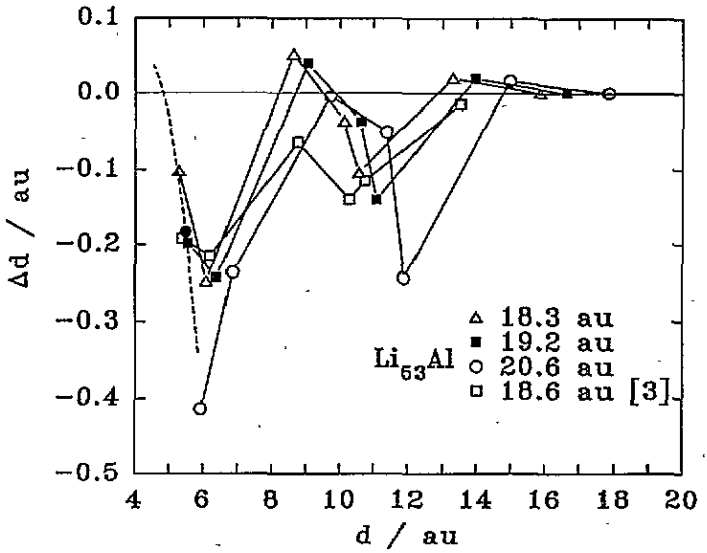

Figure 3. The corresponding data for $Li_{63}Al$ as explained in the caption of figure 1. We also include the results of Benedek *et al* [3] (white squares).

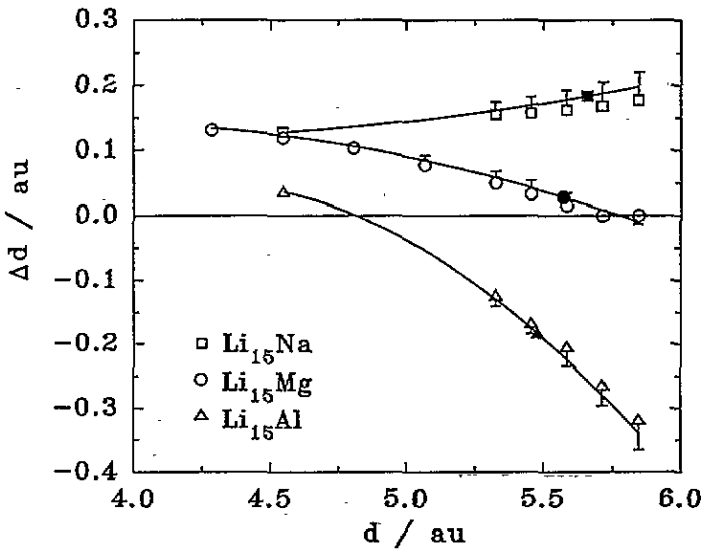

Figure 4. The displacement of the first-nearest-neighbouring shell of Li atoms around a solute atom for $Li_{15}X$ (X = Na, Mg, Al) versus the distance from an X solute atom. The error bars show the effect of the residual forces and the solid lines are simply a guide for the eye. The equilibrium lattice parameter values are shown with black symbols.

nearest-neighbouring shell of Li atoms around the solute atom is similar to that obtained in the 16-site supercell calculations. The first-nearest-neighbouring atomic shell around the solute atom relaxes outward from Na and Mg solutes and toward an Al solute in the

equilibrium case (see also figure 4).

Using a larger supercell it is possible to investigate the long-range character of the lattice relaxation. As figure 1 shows, the Na impurity induces an outward relaxation in all its neighbours and this relaxation decreases monotonically up to the fourth neighbour. Contrary to those of Na, Mg and Al impurities induce a wavelike relaxation whose amplitude decreases with increasing distance from the impurity atom. Considering the total relaxation within the unit cell, figures 1–3 show that it is positive for Na, approximately zero for Mg (positive and negative parts cancel each other) and negative for Al. In the following, the atomic displacements around a solute atom defect are discussed by considering the number of valence electrons, the electronegativity and atomic size of the different solutes and Li. Since a Na atom has one valence electron and the electronegativities of Na and Li are almost equal, the electronic environment of Li atoms does not change much when alloying Li with Na. The calculated atomic volume of bulk Na is about 75% larger than that of Li, thus leading to an almost monotonically decreasing influence on displacements, as a function of distance from a Na impurity. The number of valence electrons and the electronegativity increase in the order Na–Mg–Al, thus giving rise to an increase in the wavelike and long-range nature of the relaxation in the corresponding alloys. Due to the long-range electrostatic interaction, the range and intensity of the oscillations of the lattice distortion around an Al solute atom are larger than those in the case of a Mg solute. The total relaxation in $Li_{53}Mg$ and $Li_{53}Al$ systems adapts qualitatively to the atomic size differences in the bulk environment (atomic volume of BCC Mg is about 14% larger and FCC Al about 16% smaller than that of BCC Li).

In figure 3 are also included the results of Benedek *et al* [3] which agree reasonably well with the present results, except in the case of the fifth neighbour. The differences between their results and ours are likely to be due to the fact that we have used the partial core correction for Li, which is expected to improve the values of quantities that depend on the equilibrium lattice parameter. Furthermore, we have used four special k-points in the SC IBZ whereas Benedek *et al* used a single special k-point only.

3.2. Lattice distortion under pressure

In our previous study [13] on a 16-site supercell, the displacement of the first-nearest-neighbouring shell of Li atoms surrounding a solute atom was presented with quite a wide range of lattice parameters for $Li_{15}Mg$. In the other two cases (Li–Na and Li–Al), only a few lattice parameters around the equilibrium value were used. In the present paper we show the results for Li–Na and Li–Al in the same range of lattice parameters as for Li–Mg (see figure 4). In the case of Li–Na there was no such clear behaviour in the solute-atom-induced lattice distortion as a function of pressure, a finding which gave rise to a more precise investigation. There are always minor forces left after the relaxation procedure and the influence of these forces on the displacements might be quite pronounced. In figure 4 there is an estimation of the effect of the residual forces based on the knowledge of the forces in the ideal BCC structure and on the residual forces and displacements in the optimized structure. As can be seen, the displacement of Li atoms surrounding a Na solute decreases as a function of pressure within the whole range of the pressure investigated. Our earlier prediction of a faint increase at higher pressures [13] was based, however, on too short a range of lattice parameters around the equilibrium value. Another interesting observation is that the effect of the residual force is more pronounced in the large lattice parameters than in the small ones. An explanation for this is that the more the pressure increases the harder the material becomes, the bigger the force needed to move the atoms, and the larger the convergence criterion for forces that can be chosen. In order to obtain results that

would have the same accuracy in the structure determination within the whole investigated pressure range, the convergence criterion for forces should be chosen so that it is tighter for large lattice parameters than for small ones.

In the following, the pressure dependence of a solute-atom-induced lattice relaxation is considered for the 54-site supercell. It has been found that this pressure dependence differs considerably from impurity to impurity. It becomes stronger in the order Na–Mg–Al. The behaviour of the distortion under pressure seems to follow the hardness of the pure components. In the case of Li–Na the first-nearest-neighbouring Li shell moves toward a Na atom as pressure increases in both unit cells used, while in the Li–Mg and Li–Al systems, this shift is outward from the corresponding solute atom. Figure 1 shows that in $Li_{53}Na$ the effect of pressure on the displacements of different atomic shells decreases with increasing distance from a Na solute atom. In $Li_{53}Mg$ and $Li_{53}Al$, the position of certain neighbours depends considerably on pressure, while the position of the other neighbours is practically invariant under pressure change. The sequences of these active (A) and inactive (I) spheres are AAIIAI and AIAIAI for Mg and Al impurities, respectively. In the case of Mg and Al, the pressure dependence of the relaxation is strongest for the first-nearest-neighbouring Li shell, and for Al the effect of pressure is so strong that the order of relaxation of the first- and second-nearest-neighbours changes when pressure is varied.

The relaxations under pressure in the 54- and 16-site supercells can be compared to each other by considering the relaxations of the first-nearest-neighbouring Li shells around an impurity atom. The pressure dependence of the relaxation of the first-nearest neighbour in the 16-site unit cell is qualitatively consistent with that of the first-nearest neighbour in the 54-site unit cell in all cases investigated, except that the zero-pressure values are different. The similarities in the behaviour of lattice distortion in the 16- and 54-site supercells for Li–Mg and Li–Al may be accidental because of the long-range character of the relaxation and due to a feedback effect that the displacements of the other neighbours have on the relaxation of the first-nearest neighbour. The coincidence of the distortions of the first-nearest neighbours for $Li_{53}Al$ and $Li_{15}Al$ may also be due to strong interaction between Li and Al atoms. Thus, the bond length between an Al atom and the first-nearest-neighbouring Li atom may be nearly independent of the choice of unit cell. Summarizing from the above, the 16-site supercell is too small to avoid interaction between nearest-neighbouring solute atoms, but it is quite obvious that the 16-site supercell is large enough if we are only interested in the qualitative effects of an isolated impurity.

3.3. Equilibrium volume and bulk modulus

In our previous study [13] we considered in more detail the effects of alloying on equilibrium volume and bulk modulus. However, a new aspect emerging from the present study is the behaviour of these quantities with respect to solute atom concentration. The effects of alloying on average atomic volume and bulk modulus in the 54-site supercell are qualitatively the same as in the 16-site supercell, only smaller in magnitude, which is to be expected due to the dilution of the solution. Furthermore, the results of the 54-site supercell calculations show the importance of lattice relaxation as we already pointed out in the previous study on the 16-site supercell.

In figure 5, average atomic volume and bulk modulus for Li–X systems are presented with respect to pure Li as a function of the concentration of the solution. As can be seen, the qualitative behaviour of average atomic volume and bulk modulus of Li–Mg alloys agrees well with the experimental results [32]. The calculated absolute value of the average atomic volume and bulk modulus for pure Li are 9% smaller and 14% larger, respectively, than the

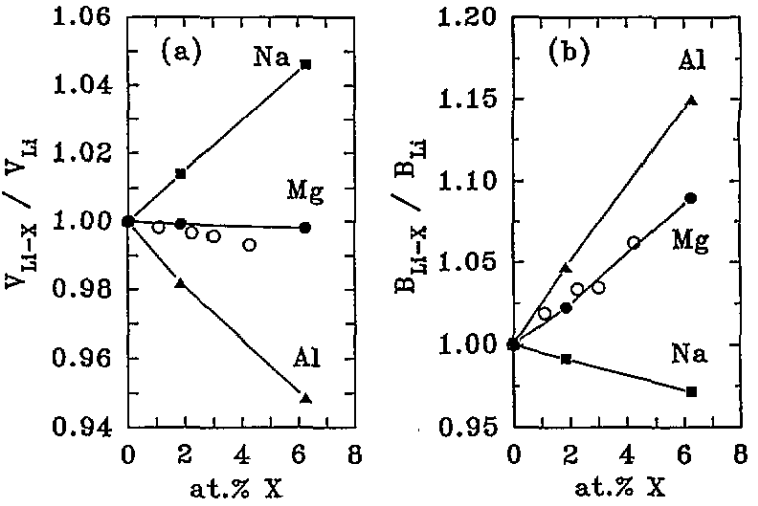

Figure 5. The average atomic volume (a) and bulk modulus (b) for Li–X dilute alloys with respect to pure Li as a function of solute concentration. The calculated absolute values for Li_{54} are $V = 133.5$ au^3 and $B = 0.137$ Mbar. We also present the experimental data for dilute Li–Mg alloys found in the literature [32] (open circles).

experimental data at room temperature. Compared with the zero-temperature values [33–35], the calculated bulk modulus of Li is only 5–9% larger. The effect of pressure on bulk modulus has also been calculated. The first derivative of bulk modulus with respect to pressure in zero pressure is quite large and the obtained value of 3.3 for Li agrees very well with the experimental data [33, 34].

3.4. Heat of formation

The solubility of Mg in BCC Li is quite high (70 at.% Mg in BCC Li), whereas the solubility of Al is limited to a narrow region. However, two intermediate compounds ($AlLi_2$ and AlLi) are known. The solubility of Na in Li is reported to be negligible and no intermediate phases are known. In our calculations, the interaction between an Al solute atom and Li solvent atoms is attractive and quite strong agreeing with the tendency of Li–Al alloys to form ordered structures. Contrary to this, the interaction between Mg and Li atoms is weak. Therefore, Li and Mg atoms are not expected to be arranged in an ordered way, thus leading to disordered structures. The interaction between Na and Li is repulsive and strong which suggests the non-solubility of these elements. All this agrees qualitatively with the above-mentioned experimental results [36].

The relevant observational quantity related closely to solubility is heat of formation which can be determined as follows [37]

$$E_f = E(\mathrm{Li}_{N-1}\mathrm{X}) - \frac{N-1}{N}E(\mathrm{Li}_N) - E(\mathrm{X})$$

where N is the number of atoms in the supercell and where $E(\mathrm{X})$ is the total energy of pure metal X with an assumption of a BCC lattice for Na and Mg, and an FCC lattice for Al. Although the correct ground state structure for Mg is HCP, the BCC structure can be used in this case since the energy difference between BCC and HCP structures is only about

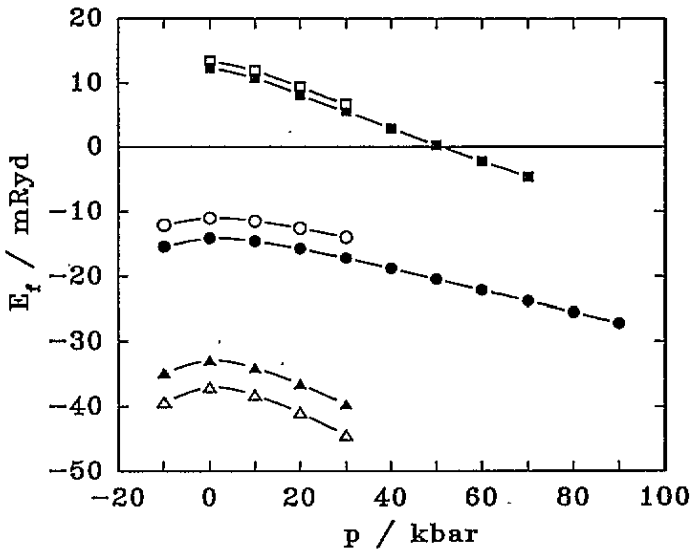

Figure 6. The heat of formation for Li–Na (squares), Li–Mg (circles) and Li–Al (triangles) as a function of pressure with 16-site (full symbols) and 54-site (open symbols) supercells.

0.4 mRyd [38], thus having a negligible influence on the formation energy of Li–Mg alloys. The calculated values of heat of formation are shown in figure 6.

The heats of formation for the 16- and 54-site supercells are comparable with each other since the errors in the first two terms on the right-hand side of the equation above almost cancel each other and the third term is the same in both cases. The heat of formation for a Na solute is distinctly positive in both cases, thus agreeing with the reported negligible solubility. For Mg the heat of formation is negative and it decreases as the Mg concentration increases in agreement with the experimental data of solubility. The heat of formation for Al is more negative than that for Mg which contradicts the experimental determination of solubilities. The explanation for this might be that the calculations for Li–Mg alloys have been made with an ordered structure while these alloys are disordered in nature. However, our results agree qualitatively with other calculated results of the heats of solution for liquid binary Li alloys [39]. When the Al concentration increases, the heat of formation becomes less negative which can be understood as follows. The interaction between Al and Li atoms is strong giving rise to a pronounced lattice relaxation. In dilute Li–Al alloys there are enough 'freely' moving Li atoms which can respond to this relaxation, but as the Al concentration increases, more of the Li atoms are pinned to other Al atoms and they are no longer free to relax. Thus, it seems that the only Li–Al alloys that exist are dilute primary alloys.

There are two kinds of effect that can be considered when the supercell size is increased: on one hand how electronic properties change and on the other hand how structural relaxation changes with respect to the solute atom concentration. When studying an ideal BCC structure it is possible to get information about the electronic effect without relaxation. In these Li alloys, when the size of the supercell is increased from 16 to 54 atoms, the heat of formation is increased by 2–3 mRyd. This value is a little larger than the vacancy-formation energy difference between the 16- and 54-site supercells of Li [1]. The effect of relaxation as a function of supercell size is not so clear since the optimized structures also include the

electronic effect. This combined effect on the heat of formation (see figure 6) is largest for Li–Al (about 5 mRyd) but opposite in sign when compared to that for Li–Mg (3 mRyd) and Li–Na (1 mRyd). Thus the 16-site supercell is not large enough for studying the effects of isolated impurities on different physical quantities at the quantitative level.

Altogether, it is important to take into account the lattice relaxation when calculating the heat of formation. If the solute atom induces a lattice relaxation of the same order as Na and Al in Li, the effect of the relaxation on the heat of formation can be as great as 40%. The heat of formation under pressure has also been calculated. In all cases investigated, the heat of formation decreases as a function of pressure which means that the heat of formation of Li–Na alloys is expected to change its sign when pressure is increased. Figure 6 presents the heat of formation for Li–X alloys as a function of pressure, showing that the heat of formation of $Li_{15}Na$ is negative above 50 kbar, indicating the possible solubility of Na in BCC Li with increasing pressure.

4. Summary

In this paper, we have studied the effects that the lattice distortion around a solute atom has on the cohesive properties of BCC Li using the first-principles structural optimization method. Although the relaxations of the first-nearest-neighbouring Li shell around the solute atom are similar in 16- and 54-site unit cells, the 16-site supercell is, however, far too small to prevent interaction between nearest-neighbouring solute atoms. The obtained results for various properties of Li alloys show that it is necessary to include an accurate solute-atom-induced lattice distortion properly in calculations if the effects of alloying are to be studied at the quantitative level.

According to our results, the interaction between Na and the first-nearest-neighbouring Li atoms is repulsive and quite strong and, in addition, the heat of formation for a Na solute is distinctly positive, thus agreeing with the reported negligible solubility. Contrary to this, the interaction between Mg and the first-nearest-neighbouring Li atoms is weak and the heat of formation for Mg is negative. Therefore, Li and Mg atoms are not expected to be arranged in an ordered way, but to form disordered alloys. The interaction between Al and the first-nearest-neighbouring Li atoms is attractive and strong and the heat of formation for Al is negative, giving rise to a tendency for Li–Al alloys to form ordered structures. All this agrees qualitatively with the experimental results of solubility for these elements [36]. The heat of formation under pressure has also been calculated. In all cases investigated, the heat of formation decreases as a function of pressure, e.g. the heat of formation for $Li_{15}Na$ is negative above 50 kbar indicating the possible solubility of Na in BCC Li under pressure. The dependence of some quantities on solute atom concentration has also been deduced from the present data. For instance, the calculated bulk modulus and average atomic volume of dilute Li–Mg alloys as a function of Mg concentration agree well with the corresponding experimental data.

The present study deals only with symmetric lattice distortions around a solute atom. Besides symmetric relaxations, it would also be interesting to study off-centre displacements of the solute atoms [40], the possibility of other energetically stable structures, and energy relations in diffusion processes [41, 42] in the investigated alloys. Moreover, the determination of different elastic constants would tell a great deal about the accuracy of the lattice optimization method used in this work. However, in these kinds of studies, the need for computer memory and CPU time increases significantly due to the lack of inversion symmetry in the system to be investigated.

Acknowledgments

We gratefully acknowledge Professor K Terakura and his research group for the molecular dynamics program. The calculations were made using the computational facilities provided by the Centre for Scientific Computing Ltd, Espoo, Finland. This work was supported by the Academy of Finland.

References

[1] Pawellek R, Fähnle M, Elsässer C, Ho K-M and Chan C-T 1991 *J. Phys.: Condens. Matter* **3** 2451–5
Frank W, Breier U, Elsässer C and Fähnle M 1993 *Phys. Rev.* B **48** 7676–8
[2] Abrikosov I A, Vekilov Yu H, Korzhavyi P A, Ruban A V and Shilkrot L E 1992 *Solid State Commun.* **83** 867–70
[3] Benedek R, Yang L H, Woodward C and Min B I 1992 *Phys. Rev.* B **45** 2607–12
[4] Cho J-H, Ihm S-H and Kang M-H 1993 *Phys. Rev.* B **47** 14 020–2
[5] Rahman S M M and Karaoglu B 1993 *J. Phys.: Condens. Matter* **5** 851–60
[6] Rajput S S, Prasad R, Singru R M, Triftshäuser W, Eckert A, Kögel G, Kaprzyk S and Bansil A 1993 *J. Phys.: Condens. Matter* **5** 6419–32
[7] Rajput S S, Singru R M and Prasad R 1994 *Solid State Commun.* **90** 339–42
[8] Arya A, Das G P, Salunke H G and Banerjee S 1994 *J. Phys.: Condens. Matter* **6** 3389–402
[9] Cho J-H and Kang M-H 1994 *Phys. Rev.* B **49** 9555–9
[10] Car R and Parrinello M 1985 *Phys. Rev. Lett.* **55** 2471–4
[11] Jost J, Heydt D, Spehr J and Ruppersberg H 1994 *J. Phys.: Condens. Matter* **6** 321–6
[12] Salo P T and Kokko K 1993 *J. Phys.: Condens. Matter* **5** 3325–32
[13] Kokko K, Salo P T and Mansikka K 1994 *Comput. Mater. Sci.* **2** 261–9
[14] Hohenberg P and Kohn W 1964 *Phys. Rev.* **136** B864–71
[15] Kohn W and Sham L J 1965 *Phys. Rev.* **140** A1133–8
[16] Wigner E 1934 *Phys. Rev.* **46** 1002
[17] Bachelet G B, Hamann D R and Schlüter M 1982 *Phys. Rev.* B **26** 4199–228
[18] Hamann D R 1989 *Phys. Rev.* B **40** 2980–7
[19] Kleinman L and Bylander D M 1982 *Phys. Rev. Lett.* **48** 1425–8
[20] Louie S G, Froyen S and Cohen M L 1982 *Phys. Rev.* B **26** 1738–42
[21] Kobayashi K, Morikawa Y, Terakura K and Blügel S 1992 *Phys. Rev.* B **45** 3469–84
[22] Williams A R and Soler J 1987 *Bull. Am. Phys. Soc.* **32** 562
[23] Štich I, Car R, Parrinello M and Baroni S 1989 *Phys. Rev.* B **39** 4997–5004
[24] Hellmann H 1937 *Einführung in die Quantenchemie* (Leipzig: Deuticke)
Feynman R P 1939 *Phys. Rev.* **56** 340–3
[25] Kobayashi K 1990 *PhD Thesis* University of Tokyo
[26] Morikawa Y 1994 *PhD Thesis* University of Tokyo
[27] Chadi D J and Cohen M L 1973 *Phys. Rev.* B **8** 5747–53
[28] Fu C-L and Ho K-M 1983 *Phys. Rev.* B **28** 5480–6
[29] Elsässer C, Fähnle M, Chan C T and Ho K M 1994 *Phys. Rev.* B **49** 13 975–8
[30] Salo P T, Kokko K, Mansikka K and Laihia R 1994 *Report Series, Department of Physics, University of Turku* R 22
[31] Banerjea A and Smith J R 1988 *Phys. Rev.* B **37** 6632–45
[32] Trivisonno J and Smith C S 1961 *Acta Metall.* **9** 1064–71
[33] Day J P and Ruoff A L 1974 *Phys. Status Solidi* a **25** 205–13
[34] Felice R A, Trivisonno J and Schuele D E 1977 *Phys. Rev.* B **16** 5173–84
[35] Anderson M S and Swenson C A 1985 *Phys. Rev.* B **31** 668–80
[36] Pearson W B 1958 *A Handbook of Lattice Spacings and Structures of Metals and Alloys* (Belfast: Pergamon)
[37] Masuda-Jindo K and Terakura K 1989 *Phys. Rev.* B **39** 7509–16
[38] Skriver H L 1982 *Phys. Rev. Lett.* **49** 1768–72
[39] Miedema A R, de Châtel P F and de Boer F R 1980 *Physica* B **100** 1–28
[40] Zunger A private communication
[41] Körblein A, Heitjans P, Stöckmann H-J, Fujara F, Ackermann H, Buttler W, Dörr K and Grupp H 1985 *J. Phys. F: Met. Phys.* **15** 561–77
[42] Kishio K and Brittain J O 1979 *J. Phys. Chem. Solids* **40** 933–40